Artificial bee colony optimized controller for unmanned rotorcraft pendulum

Sun Changhao and Haibin Duan
Science and Technology on Aircraft Control Laboratory, School of Automation Science and Electrical Engineering, Beihang University (BUAA), Beijing, People's Republic of China

Abstract

Purpose – The purpose of this paper is to propose a new algorithm for pendulum-like oscillation control of an unmanned rotorcraft (UR) in a reconnaissance mission and improve the stabilizing performance of the UR's hover and stare.

Design/methodology/approach – The algorithm is based on linear-quadratic regulator (LQR), of which the determinable parameters are optimized by the artificial bee colony (ABC) algorithm, a newly developed algorithm inspired by swarm intelligence and motivated by the intelligent behaviour of honey bees.

Findings – The proposed algorithm is tested in a UR simulation environment and achieves stabilization of the pendulum oscillation in less than 4s.

Research limitations/implications – The presented algorithm and design strategy can be extended for other types of complex control missions where relative parameters must be optimized to get a better control performance.

Practical implications – The ABC optimized control system developed can be easily applied to practice and can safely stabilize the UR during hover and stare, which will considerably improve the stability of the UR and lead to better reconnaissance performance.

Originality/value – This research presents a new algorithm to control the pendulum-like oscillation of URs, whose performance of hover and stare is a key issue when carrying out new challenging reconnaissance missions in urban warfare. Simulation results show that the presented algorithm performs better than traditional methods and the design process is simpler and easier.

Keywords Aircraft, Programming and algorithm theory, Controllers, Oscillations, Unmanned rotorcraft, Pendulum oscillation, Artificial bee colony, Linear quadratic regulator

Paper type Research paper

Introduction

Micro aerial vehicles (MAVs), essentially small scale flying robots, became an area of interest in the aerospace community with the initiation of the micro UAV (MUAV) program by Defense Advanced Research Projects Agency (DARPA) (Month *et al.*, 2004). The technological feasibility of MAVs as one possible solution to new challenging reconnaissance mission scenarios in urban warfare (local, close-up range, hidden reconnaissance, operation between obstacles and maybe even inside buildings) is depending on a bunch of questions, which are only partly answered so far.

One of the challenging problems for MAVs is to design a robust flight control system for such a miniaturized "bird", which is generally one order of magnitude smaller than any today's operational unmanned aerial vehicle (UAV) (Fu *et al.*, 2012). Richard and Stefan (2004) put forward several unique, very challenging operational requirements associated with the guidance, navigation and control of an MAV, which in combination and at the scale of an MAV sound rather futuristic. A simple, nonlinear closed-loop control law was designed for the dynamics along the vertical and pitch axis of a flapping-wing MAV, allowing an efficient stabilization of the naturally unstable model (Thomas *et al.*, 2010). The aerodynamic modelling of a ducted fan vertical take off and landing (VTOL) UAV and the problem of attitude stabilization was studied when the vehicle is remotely controlled by a pilot in presence of crosswind (Pflimlin *et al.*, 2010).

The recent boom of bio-inspired algorithms, which are derived from biological inspired self-organized systems as found in biological evolution, forging insects (ants, bees, etc.), and flocking birds and attack activities (bees, wasps, etc.), has attracted increasingly more researchers to the field of applying such intelligent approaches to optimization problems in modelling and control of UAVs (Duan and Li, 2012). A parallel hybrid algorithm for solving global optimization problems is proposed (Velazquez *et al.*, 2010), which is based on the coupling a stochastic global (simultaneous perturbation stochastic approximation, simulated annealing, and genetic algorithms (GAs)) and a local method (Newton-Krylov Interior-Point) via a surrogate model, and solved the wing modelling problem of an MAV. The hybrid algorithm combined the advantages of more than one computing methods and greatly improved the global search ability. Zhou *et al.* (2012) combined ant colony optimization (ACO) with Voronoi diagram and developed an efficient route planning method for UAVs. A new variant of particle swarm optimization (PSO), named phase angle-encoded and quantum-behaved particle swarm optimization (θ-PSO), was developed (Fu *et al.*, 2012). Due to

The current issue and full text archive of this journal is available at **www.emeraldinsight.com/1748-8842.htm**

Aircraft Engineering and Aerospace Technology: An International Journal
85/2 (2013) 104–114

[DOI 10.1108/00022661311302715]

This work was partially supported by Natural Science Foundation of China (NSFC) under grants #61273054, #60975072 and #60604009, Program for New Century Excellent Talents in University of China under grant #NCET-10-0021 and Beijing NOVA Program Foundation of China under grant #2007A017. The authors also want to thank the anonymous referees for their valuable comments and suggestions, which led to the better presentation of this work.

the incorporation of phase angle code and quantum behavior, the θ-PSO demonstrated excellent performance in planning a sage and flyable path for UAVs when compared with five other population-based algorithms.

Hover and stare is a key issue to the performance of MAVs and similar kinds of unmanned vehicles, which are designed to perform surveillance and reconnaissance missions. However, pendulum-like oscillation (Figure 1) triggered by external disturbances and other uncertain factors will badly impair its performance, thus resulting in blurred images or even overturn of the vehicle. As a result, control techniques of such a vehicle are becoming more and more important for their wide applications in civil and military fields. A recent thrust in the development of ducted-fan driven unmanned vehicles has initiated interest in applying bio-inspired algorithms and optimal control theory for the control of vehicles with a ducted fan during hover and stare.

The artificial bee colony (ABC) algorithm is a new optimization method, which is based on swarm intelligence and motivated by the intelligent behavior of honey bees. The ABC algorithm has been proved to possess a better performance in function optimization problem, compared with the GA, the differential evolution (DE) algorithm and the PSO algorithm (Karaboga and Basturk, 2007, 2008). The main advantage of ABC lies in that it simultaneously conducts local and global search in every iteration, and the probability of finding the optimal results is significantly increased, which can efficiently avoid local optimum to a large extent. An improved ABC optimization algorithm is developed based on chaos theory and successfully solved the UCAV path planning problem in various combat field environments (Xu and Duan, 2010).

The linear quadratic regulator (LQR) is, at its core, an automated way of finding an appropriate state-feedback controller. It takes care of the tedious work done by the control system engineer in optimizing the controller. However, the engineer still needs to specify the weighting factors and compare the results with the specified design goals. This paper focuses on a particular type of unmanned MAV, an unmanned rotorcraft (UR), which is driven by a rotor and a ducted fan (Figure 2). The UR has a symmetrical structure, consisting of a single rotor, a ducted fan, a ducted fan body, an undercarriage and a series of control planes at its bottom. Due to its special formation, the UR gains better efficiency, stability and stealth performance compared to traditional helicopters (Wang, 2009). A hybrid approach to stabilize the oscillation based on the LQR is proposed. The ABC algorithm is used for parameter optimization of weighting matrix Q in LQR, which makes controller design much easier for engineers. To the best knowledge of the authors, there is no existing literature that deals UP pendulum-like oscillation by combination of ABC and LQR. Series of simulation experiments and comparison are conducted, and the results verify the feasibility and effectiveness of our proposed approach.

The rest of the paper is organized as follows. The second section introduces the pendulum oscillation of the UR and deduces the mathematical model. The ABC algorithm, which is used as an optimizer for the controller parameters, is described in the third section. The main part of the paper follows in the fourth section, which gives a detailed description of the proposed approach to pendulum control that combines LQR and the hybrid optimization algorithm motivated by swarm intelligence. The simulation and comparison results using a UR are presented in the fifth section. The sixth section concludes the paper and future work is shown in the last section.

Mathematical model of pendulum oscillation

Nonlinear model

The pendulum of a UR can be abstracted as a system consisting of the suspension point O_h, the pendulum rod O_hO_t and the pendulum mass O_t, as shown in Figure 3 (Wang, 2009). $OXYZ$ is the ground-fixed coordinate system; $O_hx_1y_1z_1$ is a mobile ground coordinate system, with point O_h as the origin and parallel to $OXYZ$, while $O_hx_2y_2z_2$ is a pendulum-body coordinate frame, which originates from O_h and axis z_2 points downward along the pendulum rod O_hO_t. Decompose the two-dimesion pendulum oscillation to oscillation in the direction of axis X and Y, and the transition matrix T from $O_hx_2y_2z_2$ to $O_hx_1y_1z_1$ is obtained as follows:

$$T = \begin{bmatrix} \cos\theta_y & \sin\theta_x \sin\theta_y & \cos\theta_x \sin\theta_y \\ 0 & \cos\theta_x & -\sin\theta_x \\ -\sin\theta_y & \sin\theta_x \cos\theta_y & \cos\theta_x \cos\theta_y \end{bmatrix} \quad (1)$$

Suppose the position vector of the suspension point O_h in coordinate frame $OXYZ$ and the pendulum mass O_t in coordinate frame $O_hx_2y_2z_2$ are presented, respectively, as follows:

$$r_h = [x, y, z]^T, \quad r'_t = [0, 0, l]^T$$

Figure 1 Pendulum oscillations in axis *X*/pendulum oscillation in actual flight

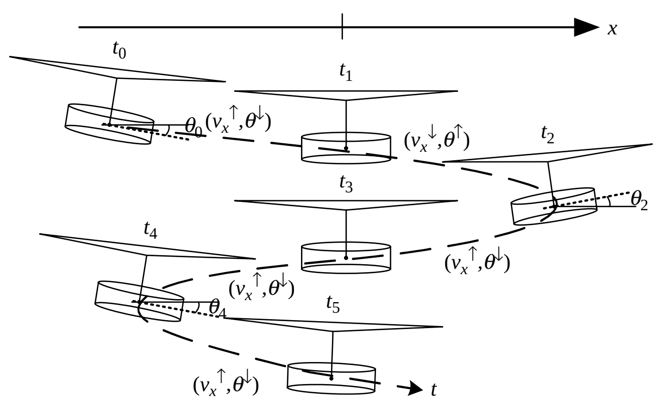

Figure 2 UR with a single rotor and ducted fan

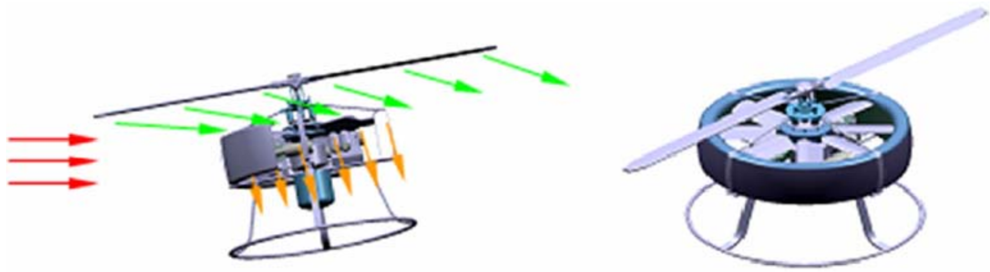

(a) (b)

Figure 3 Coordinates of the pendulum model

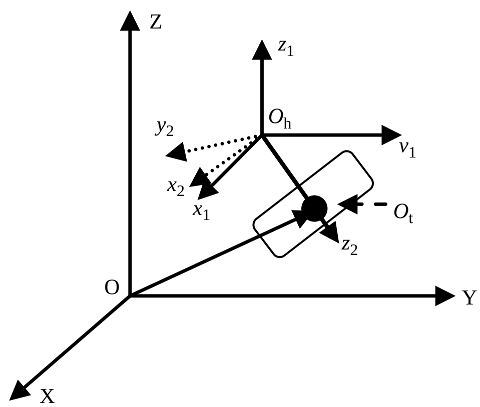

Then the coordinate of point O_t in $O_h x_1 y_1 z_1$ is calculated:

$$r_{ht} = T \cdot r_t' = [l\cos\theta_x \sin\theta_y, -l\sin\theta_x, l\cos\theta_x \cos\theta_y]^T \tag{2}$$

Finally, we have the coordinate of O_t in coordinate frame $OXYZ$ presented in equation (3):

$$r_t = r_h + T \cdot r_t' \tag{3}$$

Lagrange function of the pendulum system:

$$\begin{aligned} L &= T_0 - V = T_m + T_M' + T_M'' - V \\ &= \frac{1}{2} m\dot{r}_h^T \dot{r}_h + \frac{1}{2} m_t V_t^T V + \frac{1}{2} \mathcal{J}_{x2}\omega_{x2}^2 + \frac{1}{2}\mathcal{J}_{y2}\omega_{y2}^2 \\ &\quad - (-m_t gl\cos\theta_x\cos\theta_y + (m+m_t)(z-z_0)g) \\ &= \frac{1}{2}(m+m_t)(\dot{x}^2+\dot{y}^2+\dot{z}^2) \\ &\quad + \frac{1}{6} m_t l\left[(3+\cos^2\theta_y) l\dot{\theta}_x^2 + (1+3\cos^2\theta_x) l\dot{\theta}_y^2\right] \\ &\quad + m_t l(\dot{x}\dot{\theta}_y\cos\theta_x\cos\theta_y - \dot{x}\dot{\theta}_x\sin\theta_x\sin\theta_y - \dot{y}\dot{\theta}_x\cos\theta_x \\ &\quad - \dot{z}\dot{\theta}_x\sin\theta_x\cos\theta_y - \dot{z}\dot{\theta}_y\cos\theta_x\sin\theta_y) \\ &\quad + m_t gl\cos\theta_x\cos\theta_y - (m+m_t)(z-z_0)g \end{aligned} \tag{4}$$

where T_m, T_M', T_M'' denotes, respectively, kinetic energy of the suspension center O_h, translation kinetic energy of the pendulum mass O_t, rotational kinetic energy of the pendulum rod around the centroid of O_t, and V is potential energy of the system, setting the initial state of the pendulum oscillation as zero-potential energy surface.

Thus, equation (5) can be deduced from Lagrange equation:

$$\begin{cases} \dfrac{d}{dt}\left(\dfrac{\partial L}{\partial\dot{\theta}_x}\right) - \dfrac{\partial L}{\partial\theta_x} = 0 \\ \dfrac{d}{dt}\left(\dfrac{\partial L}{\partial\dot{\theta}_y}\right) - \dfrac{\partial L}{\partial\theta_y} = 0 \end{cases} \tag{5}$$

Considering all the above equations (1)-(5), the nonlinear mathematical model of the pendulum oscillation is finally presented in equation (6):

$$\begin{cases} \ddot{\theta}_x = (3\ddot{x}\sin\theta_x\sin\theta_y + 3\ddot{y}\cos\theta_x + 3\ddot{z}\sin\theta_x\cos\theta_y \\ \quad +2l\dot{\theta}_x\dot{\theta}_y\cos\theta_x\sin\theta_y - 3l\dot{\theta}_y^2\sin\theta_x\cos\theta_x \\ \quad -3g\sin\theta_x\cos\theta_x)/(\cos^2\theta_y+3)l \\ \ddot{\theta}_y = (-3\ddot{x}\cos\theta_x\cos\theta_y + 3\ddot{z}\cos\theta_x\sin\theta_y + 6l\dot{\theta}_x\dot{\theta}_y\sin\theta_x\cos\theta_x \\ \quad -l\dot{\theta}_x^2\sin\theta_y\cos\theta_y - 3g\cos\theta_x\sin\theta_y)/(\cos^2\theta_x+3)l \end{cases} \tag{6}$$

Table I shows the main parameters of the equivalent pendulum system structure.

Model linearization

The linear model of the pendulum phenomenon of the UR is obtained as the following procedures:

1 Change pendulum angle (θ_x, θ_y) around axis x, y to pitch and roll angle (φ_x, φ_y) according to $\varphi_x = \theta_y$, $\varphi_y = -\theta_x$, and then equation (6) is described (Jiang, 2008):

$$\begin{cases} \ddot{\phi}_y = (3\ddot{x}\sin\phi_x\sin\phi_y - 3\ddot{y}\cos\phi_y + 3\ddot{z}\sin\phi_y\cos\phi_x \\ \quad +2l\dot{\phi}_x\dot{\phi}_y\cos\phi_y\sin\phi_x - 3l\dot{\phi}_x^2\sin\phi_y\cos\phi_y \\ \quad -3g\sin\phi_y\cos\phi_y)/(\cos^2\phi_x+3)l \\ \ddot{\phi}_x = (-3\ddot{x}\cos\phi_y\cos\phi_x + 3\ddot{z}\cos\phi_y\sin\phi_x \\ \quad +6l\dot{\phi}_x\dot{\phi}_y\sin\phi_y\cos\phi_y - l\dot{\phi}_y^2\sin\phi_x\cos\phi_x \\ \quad -3g\cos\phi_y\sin\phi_x)/(\cos^2\phi_y+3)l \end{cases} \tag{7}$$

Table I Main parameters of the pendulum system structure

Symbol	Value	Physical meaning
m	10 kg	Mass of suspension centre
m_t	20 kg	Pendulum mass
l	0.86 m	Pendulum length
g	9.8 m/s^2	Gravitational acceleration
θ_x, θ_y	–	Pendulum angle around axis x, y
ϕ_x, ϕ_y	–	Pitch and roll angle
a_x, a_y	–	Suspension centre acceleration
u_x, u_y	–	Control input on O_h

2 Choose the state variables $X_e = [x, \phi_x, \dot{x}, \dot{\phi}_x, y, \phi_y, \dot{y}, \dot{\phi}_y, z, \dot{z}, \ddot{x}, \ddot{y}, \ddot{z}]^T$, input of the system $u = [\ddot{x}, \ddot{y}]^T$. Expand equation (7) into Taylor series in the vicinity of the equilibrium point and the linear model of the pendulum oscillation is finally obtained as below:

$$\begin{bmatrix} \dot{X}_x \\ \dot{X}_y \end{bmatrix} = \begin{bmatrix} A_x & 0 \\ 0 & A_y \end{bmatrix} \begin{bmatrix} X_x \\ X_y \end{bmatrix} + \begin{bmatrix} B_x & 0 \\ 0 & B_y \end{bmatrix} \begin{bmatrix} u_x \\ u_y \end{bmatrix} \tag{8}$$

where the state vector $X_x = [x, \phi_x, \dot{x}, \dot{\phi}_x]^T$, $X_y = [y, \phi_y, \dot{y}, \dot{\phi}_y]^T$, and:

$$A_x = \begin{bmatrix} 0 & 0 & 1 & 0 \\ 0 & 0 & 0 & 1 \\ 0 & 0 & 0 & 0 \\ 0 & -\frac{3g}{4l} & 0 & 0 \end{bmatrix}, \quad A_y = \begin{bmatrix} 0 & 0 & 1 & 0 \\ 0 & 0 & 0 & 1 \\ 0 & 0 & 0 & 0 \\ 0 & -\frac{3g}{4l} & 0 & 0 \end{bmatrix},$$

$$B_x = \begin{bmatrix} 0 \\ 0 \\ 1 \\ -\frac{3}{4l} \end{bmatrix}, \quad B_y = \begin{bmatrix} 0 \\ 0 \\ 1 \\ -\frac{3}{4l} \end{bmatrix}.$$

Characteristic analysis

As can be seen, oscillation in the direction of X and Y is decoupled with each other. Thus, the pendulum system is reduced to two four-order subsystems, which are independent of one another. Owing to similarity between matrix A_x and A_y, either of the two subsystems is considered to analyze characteristics of pendulum oscillation.

Considering pendulum motion only in the direction of axis X and taking actual parameters into account, the state space equation of the X-subsystem is presented as follows:

$$\begin{cases} \dot{X} = AX + BU \\ Y = CX \end{cases} \tag{9}$$

where $X = [x_1, x_2, x_3, x_4]^T = [x, \phi_x, \dot{x}, \dot{\phi}_x]^T$:

$$A = \begin{bmatrix} 0 & 0 & 1 & 0 \\ 0 & 0 & 0 & 1 \\ 0 & 0 & -0.6500 & 0.6500 \\ 0 & -8.547 & 0.5669 & -0.3924 \end{bmatrix},$$

$$B = \begin{bmatrix} 0 \\ 0 \\ 1 \\ -0.872 \end{bmatrix}, \quad C = \begin{bmatrix} 1 & 0 & 0 & 0 \\ 0 & 1 & 0 & 0 \\ 0 & 0 & 1 & 0 \\ 0 & 0 & 0 & 1 \end{bmatrix}.$$

The zero-input response of the pendulum oscillation system (9) in Figure 4 shows that the initial state triggers pendulum oscillation and the oscillation amplitude attenuates with time. Besides, the position and velocity of the suspension center also fluctuates with slight amplitude. The oscillation characteristic takes more than 20 s to die away, which inevitably leads to performance degradation such as blurred images and calls for a control system to eliminate disturbances.

ABC algorithm

ABC algorithm was first proposed by simulating the self-organization simulation model of honey bees (Seeley, 1995). In this model, although each bee only performs one single task, yet through a variety of information communication ways between bees, the entire colony can complete a number of complex works such as hives building, pollen harvest and so on. Then a bee colony optimization (BCO) algorithm was further introduced (Teodorovic and Orco, 2005). And in 2007, Karaboga and Basturk (2007) put forward an improved ABC algorithm.

Compared with conventional bio-inspired algorithms used for optimization problems, such as GA, PSO and so on, the ABC algorithm differs from them in that ABC simultaneously carries out local search and global search in the optimization space and can efficiently avoid trapping into local optimum, thus resulting in an excellent balance between exploitation and exploration, which makes ABC a more appropriate choice for parameter optimization in control system design.

Basic principles

Karlvon Frisch, a famous Nobel prize winner, once found that in nature, although each bee only performs one single task, yet through a variety of information communication ways between bees such as waggle dance and special odor, the entire colony can always easily find food resources that produce relative high amount nectar, hence realize its self-organizing behavior. In nature, the bees crawl along a straight line, and then turn left, moving as Figure 5 and swinging their belly (Fathian *et al.*, 2007; Duan *et al.*, 2010a, b). Such a dance is called waggle dance, and the angle between the gravity direction and the center axis of the dance is exactly equal to the angle between the sun and food source (Figure 5).

In addition, waggle dance of the bees can also deliver more detailed information about the food sources such as distance and direction. When bees are dancing, head up means they should fly towards the sun in order to find the food source location, while head down indicates flying backwards the sun. Besides, dancing speed of the bees is closely related with the distance between current position and food source location. The longer the distance is, the longer the time for bees swinging. Then each bee in the hive selects a food source to search for nectar, or researches new food sources around the bee hive, according to the information delivered by the other bee's waggle dance (Singh, 2009). In this way, through this kind of information exchanging and learning, the whole colony would always find relatively prominent nectar source.

In order to introduce the model of forage selection that leads to the emergence of collective intelligence of honey bee swarms, three essential components are defined: food sources, unemployed foragers and employed foragers:

1 Food sources (A and B in Figure 6): for the sake of simplicity, the "profitability" of a food source can be represented with a single quantity (Singh, 2009). In our target recognition problem, the position of a food source represents a possible parameters solution to the optimization problem and the nectar amount of a food source corresponds to the similarity value of the associated solution.
2 Unemployed foragers: if it is assumed that a bee has no knowledge about the food sources in the search field, the bee initializes its search as an unemployed forager. Unemployed foragers are continually at look out for a

Figure 4 Zero-input response curves without control

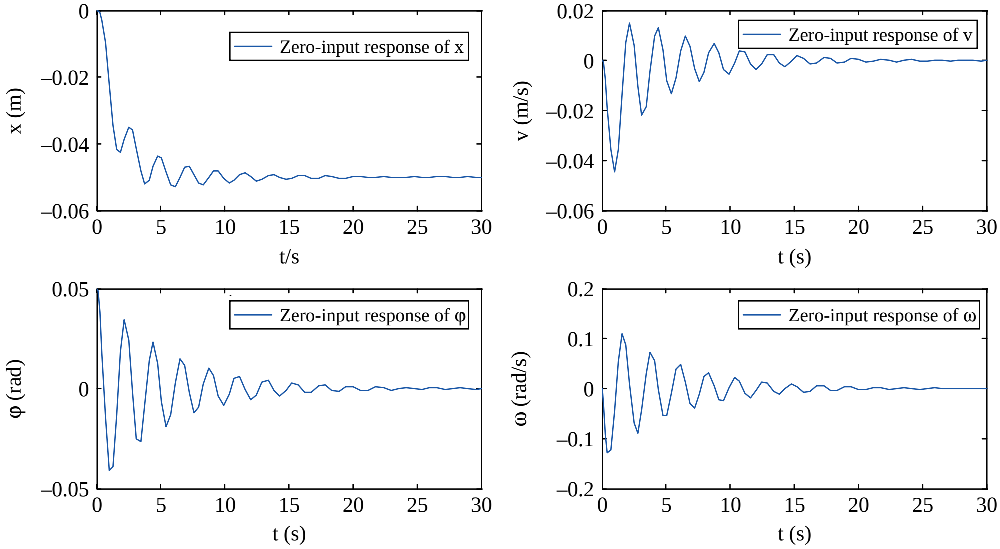

Figure 5 Waggle dances of honey bees

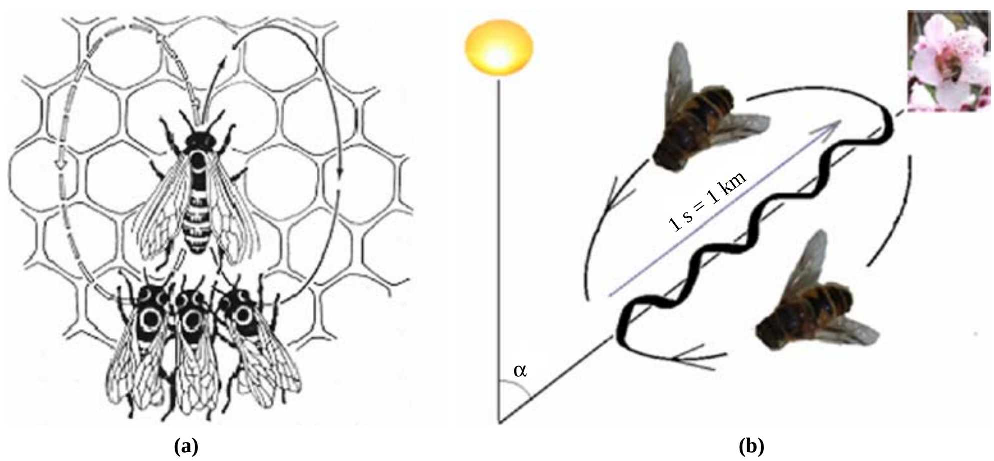

food source to exploit. There are two types of unemployed foragers: scouts and onlookers.

3 Employed foragers: they are associated with a particular food source which they are currently exploiting. They carry with them information about this particular source, the profitability of the source and share this information with a certain probability. After the employed foraging bee loads a portion of nectar from the food source, it returns to the hive and unloads the nectar to the food area in the hive.

At the initial moment, all the bees without any prior knowledge play the role of detecting bees. After a random search for bee sources, the detecting bees can convert into any kind of bees above in accordance with the profit of the searched food sources.

Mathematical description

Define N_s as the total number of bees, N_e as the colony size of the employed bees and N_u as the size of unemployed bees, which satisfy the equation $N_s = N_e + N_u$. We usually set N_e equal to N_u. D is the dimension of individual solution vector, $S = R^D$ represents individual search space, and S^{N_e} denotes the colony space of employed bees. An employed bee colony can be expressed by N_e dimension vector $\vec{X} = (X_1, \ldots, X_{N_e})$, where $X_i \in S$ and $i \leq N_e$. $\vec{X}(0)$ means the initial employed bee colony, while $\vec{X}(n)$ represents employed bee colony in the nth iteration. Denote $f : S \rightarrow R^+$ as the fitness function, and the standard ABC algorithm can be expressed as follows:

- *Step 1.* Randomly initialize a set of feasible solutions $(X_1, \ldots, X_{N_s})$, and the specific solution X_i can be generated by:

$$X_i^j = X_{\min}^j + rand(0,1)\left(X_{\max}^j - X_{\min}^j\right) \tag{10}$$

where $j \in \{1, 2, \ldots, D\}$ is the jth dimension of the solution vector. $X_{\max}^j$ means the maximum value of the jth element of a solution. By the same token, $X_{\min}^j$ means the minimum value of the jth element of a solution. $X_{\max}^j$ and $X_{\min}^j$ are problem dependent and are chosen to constrain the candidate solution in a specified search space. Calculate the fitness value of each solution vector, respectively, and set the top N_e best solutions as the initial population of the employed bees $\vec{X}(0)$:

Figure 6 The behavior of honey bee foraging for nectar

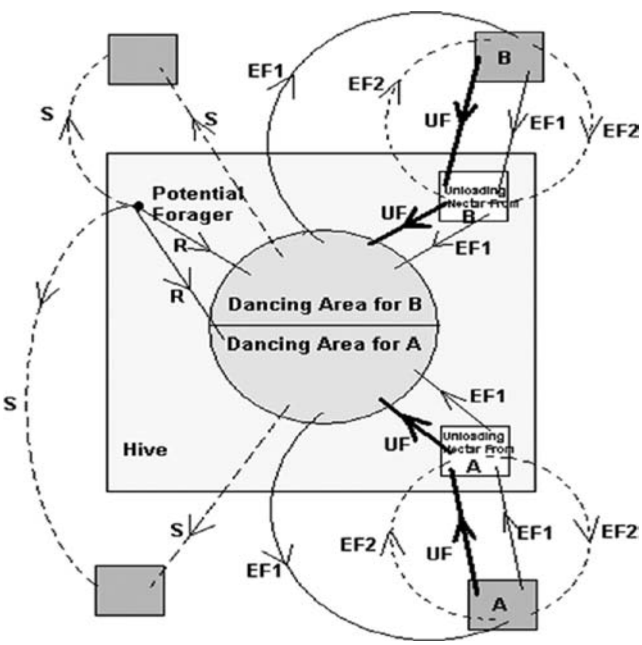

- *Step 2.* For an employed bee in the nth iteration $X_i(n)$, search new solutions in the neighborhood of the current position vector according to the following equation:

$$V_i^j = X_i^j + \varphi_i^j\left(X_i^j - X_k^j\right) \tag{11}$$

where $V \in S$, $j \in \{1, 2, \ldots, D\}$, $k \in \{1, 2, \ldots, N_e\}$, $k \neq i$, k and j are randomly generated, φ_i^j is a random number between -1 and 1.

Generally, this searching process is actually a random mapping from individual space to individual space, and this process can be denoted with $T_m : S \rightarrow S$, and its probability distribution is clearly only related to current position vector $X_i(n)$, and has no relation with past location vectors as well as the iteration number n:

- *Step 3.* Apply the greedy selection operator $T_s : S^2 \rightarrow S$ to choose the better solution between searched new vector V_i and the original vector X_i into the next generation. Its probability distribution can be described as follows:

$$P\{T_s(X_i, V_i) = V_i\} = \begin{cases} 1, & f(V_i) \geq f(X_i) \\ 0, & f(V_i) < f(X_i) \end{cases} \tag{12}$$

The greedy selection operator ensures that the population is able to retain the elite individual, and accordingly the evolution will not retreat. Obviously, the distribution of T_s is has no relation with the iteration n:

- *Step 4.* Each unemployed bee selects an employed bee from the colony according to their fitness values. The probability distribution of the selection operator $T_{s1} : S^{N_e} \rightarrow S$ can described as follows:

$$P\{T_{s1}(\vec{X}) = X_i\} = \frac{f(X_i)}{\sum_{m=1}^{N_e} f(X_m)} \tag{13}$$

- *Step 5.* The unemployed bee searches in the neighborhood of the selected employed bee's position to find new solutions. The updated best fitness value can be denoted with *f_best*, and the best solution parameters can be expressed by $(x_1, x_2, \ldots, x_D)$.
- *Step 6.* If the searching times surrounding an employed bee *Bas* exceeds a certain threshold *Limit,* but still could not find better solutions, then the location vector can be re-initialized randomly according to the following equation:

$$\mathrm{X_i}(n+1) = \begin{cases} X_{\min} + rand(0,1)(X_{\max} - X_{\min}), & Bas_i \geq Limit \\ X_i(n), & Bas_i < Limit \end{cases} \tag{14}$$

- *Step 7.* If the iteration value is larger than the maximum number of the iteration (that is, $T > T_{\max}$), output the optimal fitness value *f_best* and correlative parameters $(x_1, x_2, \ldots, x_D)$. If not, go to Step 2.

Step 6 is a most prominent aspect making ABC algorithm different from other algorithms, which is designed to enhance the diversity of the population to prevent the population from trapping into the local optimum (Duan *et al.*, 2010a, b). Obviously, this step can improve the probability of finding the best solution efficiently, and make the ABC algorithm perform much better. The flow chart of the basic ABC algorithm is given in Figure 7.

Proposed controller

LQR is about how to select an appropriate control vector $u(t)$ so that the given quadratic performance index, equation (15), obtains the minimum value. It is proved that the performance index (15) shall reach its minimum by means of linear control law in equation (16):

$$\mathcal{J} = \int_0^\infty (X^T QX + u^T Ru)dt \tag{15}$$

$$u(t) = -KX(t) = R^{-1}B^T PX(t) \tag{16}$$

and the optimal matrix P can be calculated from Algebraic Riccati equation:

$$A^T P + PA - PBR^{-1}B^T P + Q = 0 \tag{17}$$

Taking all factors into account, including performance of the control system and restrictions on the total energy consumed, matrices Q and R are chosen to have the form of:

$$Q = \mathrm{diag}(q_{11}, q_{22}, 0, 0), R = 1$$

in which parameters q_{11} and q_{22} are to be optimized to acquire desired control performance. Let input u be acceleration of the suspension center, and the corresponding pendulum-holding back control law is given in the following form:

$$\begin{aligned} u &= -KX = R^{-1}B^T PX(t) \\ &= -(k_1x_1 + k_2x_2 + k_3x_3 + k_4x_4) \end{aligned} \tag{18}$$

where the control input u is calculated from a full state feedback, of which the feedback gains $[k_1,k_2,k_3,k_4]$ are calculated from the optimized LQR.

Figure 7 Flowchart of the basic ABC algorithm

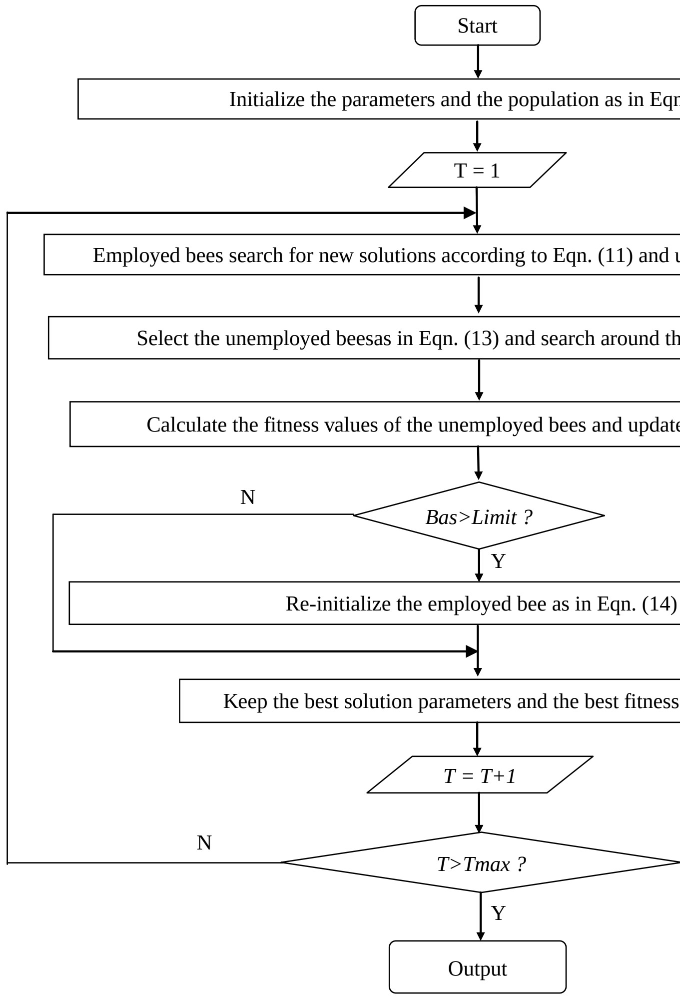

The ABC optimized control system based on LQR is demonstrated as in Figure 8. The proposed controller has a full state feedback structure, whose control input u_c is a linear combination of all the states x_1, x_2, x_3, and x_4. The feedback gains k_1, k_2, k_3, and k_4 are derived from the LQR approach, whose weighting matrix Q is optimized by ABC offline. The actual control signal acting upon the pendulum is u_a, which is the sum of x_g and u_c. Here x_g can be seen a disturbance factor. The full state feedback structure and the ABC optimized

Figure 8 Structure of pendulum-holding back system

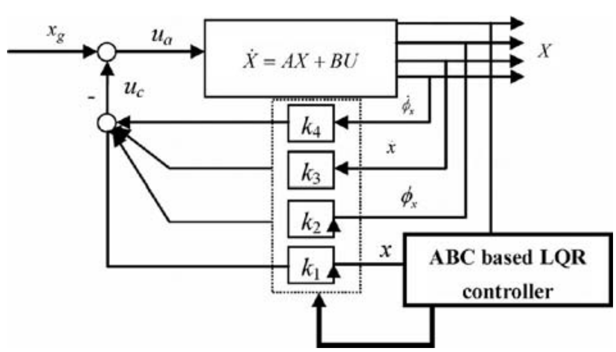

weighting matrix Q in LQR facilitate the control system design and guarantee stability of the closed loop system. Finally the actual control signal u_a is obtained by equation (18) and x_g to regulate the plant to the desired equilibrium.

The implementation procedure of our proposed ABC optimized LQR controller can be described as follows:

- *Step 1.* According to actual wind tunnel test data and main parameters of the system structure in Table I, establish the nonlinear mathematical model of pendulum oscillation (equation (6)).
- *Step 2.* Expand the nonlinear mathematical model into Taylor series in the vicinity of the equilibrium point, and obtain the linear model of the pendulum oscillation, see equation (8).
- *Step 3.* Set the performance index $\mathcal{J}$, the weighting matrices Q and R.
- *Step 4.* Optimize the designed control law using the ABC algorithm, where parameters q_{11} and q_{22} are to be optimized using the fitness function of:

$$f := 1/50^{*}\int_{0}^{\infty}(X^{T}QX + u^{T}Ru)dt$$

Aircraft Engineering and Aerospace Technology: An International Journal
Volume 85 · Number 2 · 2013 · 104–114

- *Step 5*. Solve the Algebraic Riccati equation in equation (17) and get the matrix P.
- *Step 6*. Calculate the feedback gain vector:

$$K = -R^{-1}B^TP$$

- *Step 7*. Obtain the optimized control law:

$$u = -KX = R^{-1}B^TPX(t)$$

The flow chart of the proposed controller is shown in Figure 9.

Simulation results

Assuming that the UR is executing a surveillance mission using the hover and stare mode in the actual flight environment. Due to external disturbances, take cross winds for example, the system gets an initial state $x = [0, 0.05, 0, 0]$, which would otherwise give rise to pendulum oscillation (Figure 4) without an appropriate controller.

Tables II and III show the simulation parameters of ABC and PSO, which is used for comparison to verify the feasibility of ABC. Figure 10 shows the evolution curves of

Figure 9 Procedure of our proposed method

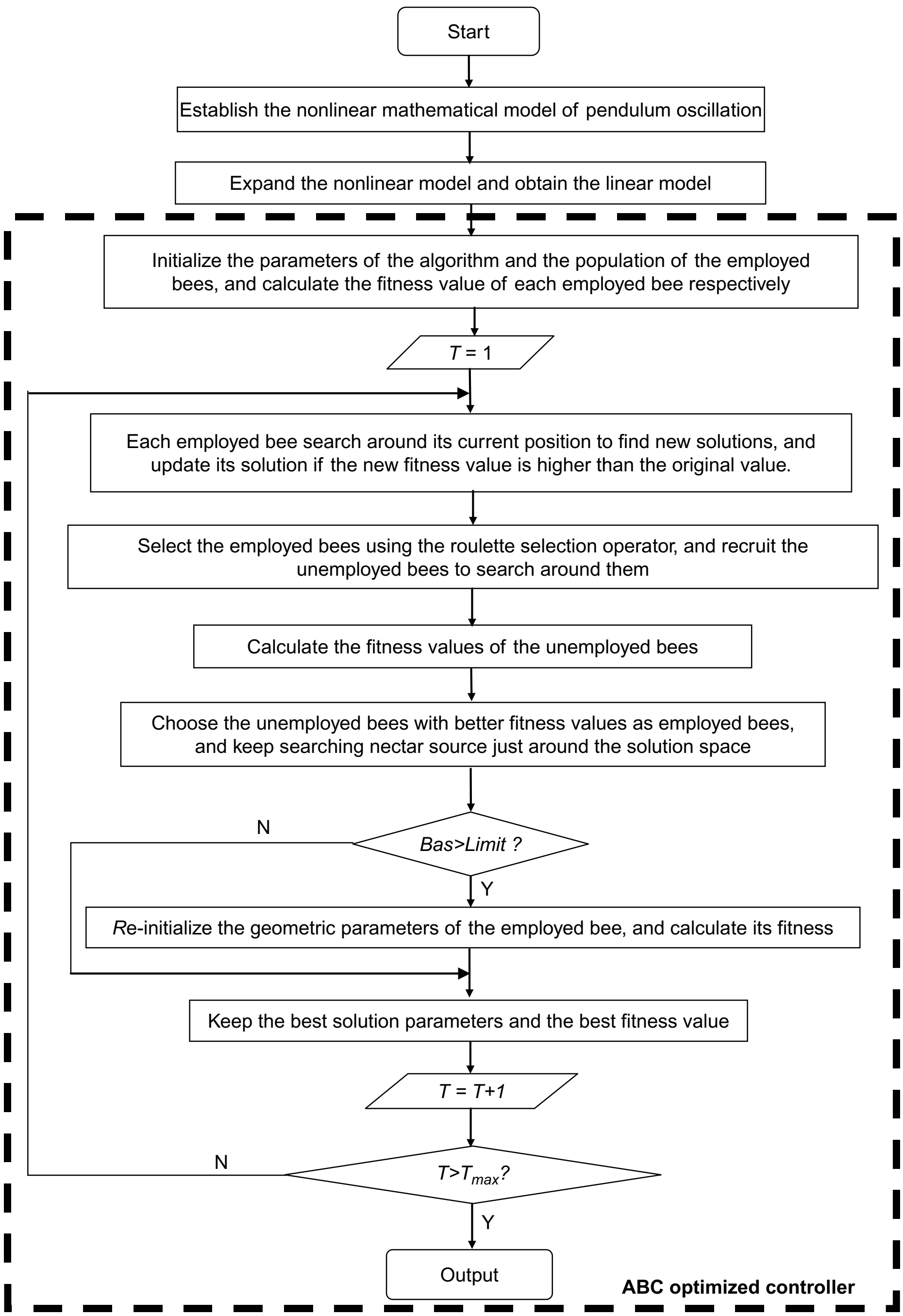

Table II Simulation parameters of ABC

Parameter	Meaning	Value
N_s	Total number of bees	20
N_e	Number of employed bees	10
N_u	Number of unemployed bees	10
D	Dimension of individual solution vector	2
Limit	Trial threshold	5
C_{max}	Stopping iteration	20
X_{max}/X_{min}	Maximum/minimum value of x	100/0.1

Table III Simulation parameters of PSO

Parameter	Meaning	Value
N	Total number of particles	20
D	Dimension of individual solution vector	2
c_1/c_2	Learning coefficient	1.8/1.3
k	Constriction factor	0.45
C_{max}	Stopping iteration	20
X_{max}/X_{min}	Maximum/minimum value of x	100/0.1

Figure 10 Evolution curves of ABC and PSO

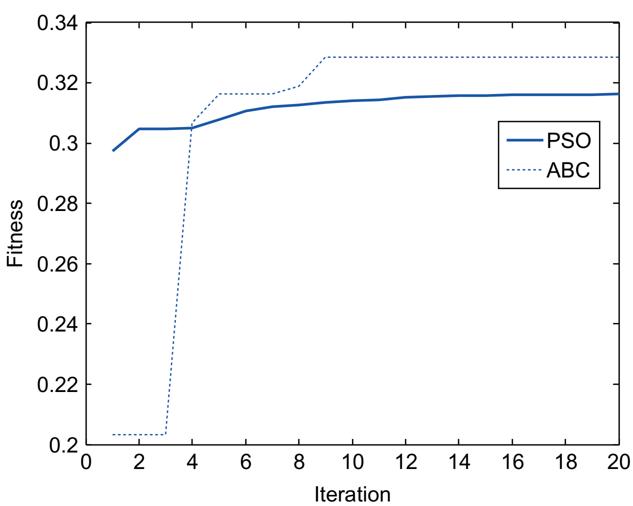

ABC and PSO, signified, respectively, by the thin dot line and the thick line. The figure demonstrates that the fitness function $f(x)$ increases as the generation iterates with time, gradually converging to an optimal result. It can be seen from the figure that ABC achieves a better result with a higher fitness value after 20 iterations of optimization, though it possesses a worse initial population due to some random reason. However, the PSO algorithm fails to find a satisfying solution of the optimization problem compared to ABC, although it has a better initialization process.

Using the ABC based LQR controller shown as in Figure 8 and experimental settings given above, control parameters which include the optimal weight matrix Q and the resulting feedback vector K are obtained as in Table IV.

The zero-input responses of the pendulum-like oscillation with an initial pendulum angle of 0.05 rad, which is brought about by cross winds in the actual flight environment, are shown in Figure 11. Compared with responses without control in Figure 4, the dynamic behaviors of x and ϕ_x state clearly that the closed loop eliminates the pendulum-like oscillation and the state converges to the equilibrium point in an average time of 6 s which shortens the stabilizing time and improves the performance of UR's hover and stare.

Table IV Control parameters of the ABC based LQR approach

Parameter	Optimized value
Q	*diag*(7.4158, 20.2363, 0, 0)
K	[8.6115, −15.6414, 6.0681, 0.5931]

Furthermore, we consider a constant interference force acting upon the pendulum system besides the initial state. Here we assume there is a strong crosswind which acts upon the vehicle body and gives rise to a constant acceleration to the UR. The resulting responses are shown in Figure 12, where the constant acceleration is taken as $0.2\,\mathrm{m/s^2}$ while the control framework and relative parameters remain the same as mentioned in Figure 8 and Table IV.

As shown in Figure 12, the ABC based LQR controller holds back the interference of the constant disturbance as well as the initial state in 6 s. The UR is stabilized to a state of $x = [0.024, 0, 0, 0]$, which means that the LQR control design technique based on ABC has a very nice robustness property and has the ability to restrain external disturbances. In this case, the UR's performance of surveillance would be improved because more accurate and clearer images are taken due to the stability improvement of the hover and stare state.

Conclusions

The performance of hover and stare is the key issue to MAVs when carrying out new challenging reconnaissance missions in urban warfare (local, close-up range, hidden reconnaissance, operation between obstacles and maybe even inside buildings). However, pendulum-like oscillation caused by uncertainty will badly impair the performance of hover and stare, resulting in blurred images or even overturn. In this paper, a novel ABC optimized approach for pendulum control in a particular kind of UR with a ducted fan is described. This method takes advantage of the optimality and accuracy of LQR, and the ABC algorithm is adopted to optimize the weighting parameters. Series of experiments are conducted. Comparison with the PSO algorithm is carried out and shows that the ABC algorithm performs better than PSO in LQR optimization for the UR pendulum control. A constant disturbance is also incorporated into the model to investigate robustness of the proposed controller. Simulation results verify the feasibility, effectiveness and robustness of our proposed approach, which provides a more effective way for control law design.

Further work

Our future work will focus on how to apply the algorithm and the control law in the actual flight of a MAV with a ducted fan and try to improve its performance.

Figure 11 Zero-input response with the proposed controller

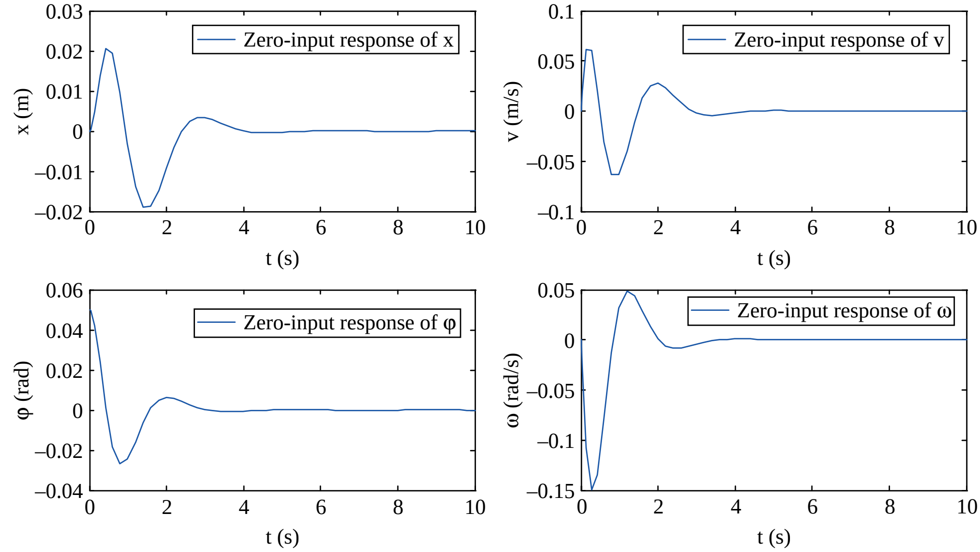

Figure 12 Responses of the pendulum system with a constant disturbance

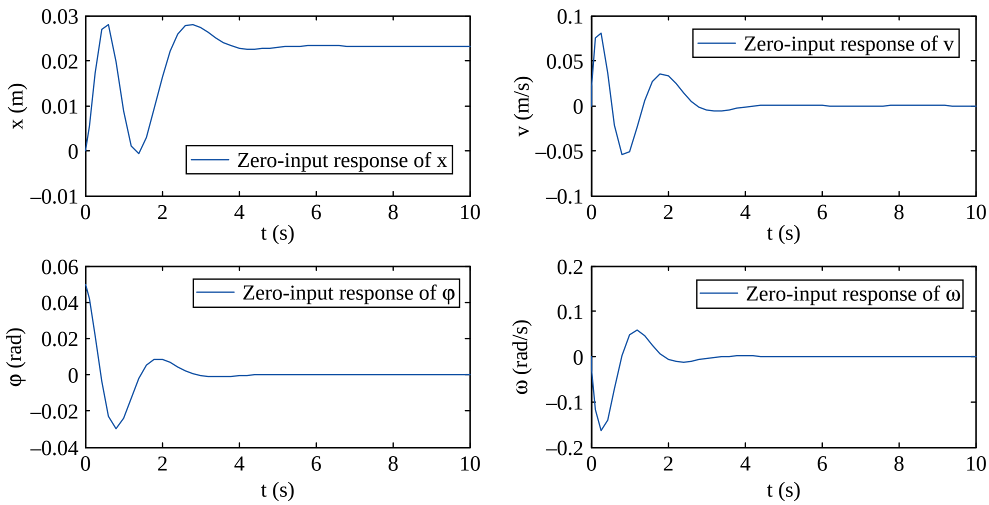

References

Duan, H.B. and Li, P. (2012), "Progress in control approaches for hypersonic vehicle", *Science China Technological Sciences*, Vol. 55 No. 10, pp. 2965-70.

Duan, H.B., Xu, C.F. and Xing, Z.H. (2010a), "Artificial bee colony optimization based quantum evolutionary for continuous optimization problems", *International Journal of Neural Systems*, Vol. 20 No. 1, pp. 39-50.

Duan, H.B., Shao, S., Su, B.W. and Zhang, L. (2010b), "New development thoughts on the bio-inspired intelligence based control for unmanned combat aerial vehicle", *Science China Technological Sciences*, Vol. 53 No. 8, pp. 2025-31.

Fathian, M., Amiri, B. and Maroosi, A. (2007), "Application of honey bee mating optimization algorithm on clustering", *Applied Math Computing*, Vol. 190 No. 2, pp. 1502-13.

Fu, J., Chen, W.H. and Qu, Q.X. (2012), "Chattering-free sliding mode control with unidirectional auxiliary surfaces for miniature helicopters", *International Journal of Intelligent Computing and Cybernetics*, Vol. 5 No. 3, pp. 421-38.

Jiang, J.Z. (2008), "Research on control technology of pendulum in single rotor helicopter with ducted fan", PhD dissertation, Nanjing University of Aeronautics and Astronautics.

Karaboga, D. and Basturk, B. (2007), "A powerful and efficient algorithm for numerical function optimization: artificial bee colony (ABC) algorithm", *Journal of Global Optimization*, Vol. 39 No. 3, pp. 459-71.

Karaboga, D. and Basturk, B. (2008), "On the performance of artificial bee colony (ABC) algorithm", *Applied Soft Computing*, Vol. 8 No. 1, pp. 687-97.

Month, J.S., Sean, S.W.S. and Mark, B.T. (2004), "A study of the control of micro air vehicles using the linear dynamic inverse approach", *Proceedings of the 1st AIAA Intelligent Systems Technical Conference, Chicago*, pp. 20-2.

Pflimlin, J.M., Binetti, P., Soueres, P., Hamel, T. and Trouchet, D. (2010), "Modeling and attitude control analysis of a ducted-fan micro aerial vehicle", *Control Engineering Practice*, Vol. 18 No. 3, pp. 209-18.

Richard, K.A. and Stefan, S. (2004), "Flight control of micro aerial vehicles", *Proceedings of AIAA Guidance, Navigation, and Control Conference and Exhibit, Providence, Rhode Island*, pp. 16-19.

Seeley, T.D. (1995), *The Wisdom of the Hive: The Social Physiology of Honey Bee Colonies*, Harvard University Press, Cambridge, MA.

Singh, A. (2009), "An artificial bee colony algorithm for the leaf-constrained minimum spanning tree problem", *Applied Soft Computing*, Vol. 9 No. 2, pp. 625-31.

Teodorovic, D. and Orco, M.D. (2005), "Bee colony optimization – a cooperative learning approach to complex transportation problems", *Proceedings of the 10th EWGT Meeting and 16th Mini EURO Conference*, pp. 51-60.

Thomas, R., Mustapha, O. and Thierry, L.M. (2010), "Longitudinal modeling and control of a flapping-wing micro aerial vehicle", *Control Engineering Practice*, Vol. 18 No. 7, pp. 679-90 (Special Issue on Aerial Robotics).

Wang, H.Q. (2009), "Research on several problems on flight control of coaxial rotor/ducted-fan unmanned helicopter", PhD dissertation, Nanjing University of Aeronautics and Astronautics.

Xu, C.F. and Duan, H.B. (2010), "Artificial bee colony optimized edge potential function approach to target recognition for low-altitude aircraft", *Pattern Recognition Letters*, Vol. 31 No. 13, pp. 1759-72.

Zhou, S.D., Wang, J. and Jin, Y.Q. (2012), "Route planning for unmanned aircraft based on ant colony optimization and Voronoi diagram", *Proceedings of International Conference on Intelligent System Design and Engineering Application (ISDEA), Sanya, Hainan*, pp. 732-5.

Further reading

Fu, Y.G. and Ding, M.Y. (2012), "Phase angle-encoded and quantum-behaved particle swarm optimization applied to three-dimensional route planning for UAV", *IEEE Transactions on Systems, Man and Cybernetics, Part A: Systems and Humans*, Vol. 42 No. 2, pp. 511-26.

Leticia, V., Miguel, A., Reinaldo, S., Carlos, R., Miguel, H., Matt, C. and Antony, J. (2010), "Hybrid optimization schemes for global optimization: wing modeling of micro-aerial vehicles", *Proceedings of 2010 DOD High Performance Computing Modernization Program Users Group Conference (HPCMP-UGC), Shaumburg, IL, USA*, pp. 149-54.

Vincent, R., Mohammed, T. and Gilles, L. (2012), "Comparison of parallel genetic algorithm and particle swarm optimization for real-time UAV path planning", *IEEE Transactions on Industrial Informatics* (in press).

About the authors

Sun Changhao is currently a PhD candidate in the School of Automation Science and Electrical Engineering, Beihang University (Beijing University of Aeronautics and Astronautics, BUAA), Beijing, China. He received his Bachelor degree in Automation Science and Technology from Beijing Institute of Technology (BIT) in 2010. His current research interests include bio-inspired computation, optimal estimation, game theory and intelligent control.

Professor Haibin Duan is currently a Full Professor in the School of Automation Science and Electrical Engineering, Beihang University (Beijing University of Aeronautics and Astronautics, BUAA), Beijing, China. He received the PhD degree from Nanjing University of Aeronautics and Astronautics (NUAA) in 2005. He was an academic visitor of National University of Singapore (NUS) in 2007, a senior visiting scholar of The University of Suwon (USW) of South Korea in 2011. He is currently an IEEE Senior Member, committee member of Guidance, Navigation and Control (GNC) Technical Committee of Chinese Society of Aeronautics and Astronautics, committee member of Chinese Association for Artificial Intelligence, and committee member of Chinese Association of Automation. He has published two monographs and over 40 peer-reviewed papers in international journals. His current research interests include bio-inspired computation, advanced flight control, and bio-inspired computer vision. Haibin Duan is the corresponding author and can be contacted at: hbduan@buaa.edu.cn